Pediatr Nephrol (2008) 23:733–741
DOI 10.1007/s00467-007-0735-4

ORIGINAL ARTICLE

Kidney cysts, pancreatic cysts, and biliary disease in a mouse model of autosomal recessive polycystic kidney disease

Scott S. Williams · Patricia Cobo-Stark · Leighton R. James · Stefan Somlo · Peter Igarashi

Received: 9 August 2007 / Revised: 26 November 2007 / Accepted: 27 November 2007 / Published online: 20 February 2008

Abstract Mutations in *PKHD1* cause autosomal recessive polycystic kidney disease (ARPKD). We produced a mouse model of ARPKD by replacing exons 1–3 of *Pkhd1* with a *lacZ* reporter gene utilizing homologous recombination. This approach yielded heterozygous $Pkhd1^{lacZ/+}$ mice, that expressed β-galactosidase in tissues where *Pkhd1* is normally expressed, and homozygous $Pkhd1^{lacZ/lacZ}$ knockout mice. Heterozygous $Pkhd1^{lacZ/+}$ mice expressed β-galactosidase in the kidney, liver, and pancreas. Homozygous $Pkhd1^{lacZ/lacZ}$ mice lacked *Pkhd1* expression and developed progressive renal cystic disease involving the proximal tubules, collecting ducts, and glomeruli. In the liver, inactivation of *Pkhd1* resulted in dilatation of the bile ducts and periportal fibrosis. Dilatation of pancreatic exocrine ducts was uniformly seen in $Pkhd1^{lacZ/lacZ}$ mice, with pancreatic cysts arising less frequently. The expression of β-galactosidase, *Pkd1*, and *Pkd2* was reduced in the kidneys of $Pkhd1^{lacZ/lacZ}$ mice compared with wild-type littermates, but no changes in blood urea nitrogen (BUN) or liver function tests were observed. Collectively, these results indicate that deletion of exons 1–3 leads to loss of *Pkhd1* expression and results in kidney cysts, pancreatic cysts, and biliary ductal plate malformations. The $Pkhd1^{lacZ/lacZ}$ mouse represents a new orthologous animal model for studying the pathogenesis of kidney cysts and biliary dysgenesis that characterize human ARPKD.

Keywords *Pkhd1* · ARPKD · Polycystic kidney disease · Biliary ductal plate malformations

S. S. Williams (✉) · P. Igarashi
Department of Pediatrics,
University of Texas Southwestern Medical Center,
5323 Harry Hines Blvd,
Dallas, TX 75390, USA
e-mail: scotts.williams@utsouthwestern.edu

P. Cobo-Stark · L. R. James · P. Igarashi
Department of Internal Medicine,
University of Texas Southwestern Medical Center,
Dallas, TX, USA

S. Somlo
Departments of Internal Medicine and Genetics,
Yale University School of Medicine,
New Haven, CT, USA

Introduction

Autosomal recessive polycystic kidney disease (ARPKD) is a monogenic disorder that is characterized by cystic kidney disease and biliary dysgenesis [1]. The kidney cysts originate from the renal collecting ducts and produce nephromegaly and chronic renal failure. Neonates with the severe perinatal form of ARPKD have a high mortality rate and present with intrauterine kidney failure, oligohydramnios, Potter's facies, and pulmonary hypoplasia. ARPKD can also present later in life with less severe cystic disease and a better prognosis. All ARPKD patients have liver involvement due to biliary dysgenesis, a ductal plate malformation characterized by aberrant development of the intrahepatic bile ducts. The liver abnormalities range from dilated, irregular bile ducts within the portal triad to more extensive disease, including hepatosplenomegaly and choledochal cysts (Caroli's disease) [2]. Over time, the liver disease progresses to periportal fibrosis and portal hypertension.

ARPKD is caused by mutations in *PKHD1* (polycystic kidney and hepatic disease 1) [3, 4]. Mutations have been found throughout the gene, and genotype–phenotype correlations have revealed that the presence of two truncating mutations causes perinatal lethal disease, where-

as missense mutations are associated with longer-term survival [5]. The human *PKHD1* gene is located on chromosome 6 and consists of 67 exons, with the longest open reading frame extending over 12 kb. The orthologous mouse *Pkhd1* transcript is ~14 kb and contains a start codon in exon 2. Although exons 1 and 2 have no homology to the human gene, exon 3 contains the site of one of the most common human mutations, T36M, and shows 91% homology to the human gene [4].

The function of the protein product of *Pkhd1*, called fibrocystin or polyductin, remains unclear. Its predicted structure suggests that it is a membrane protein similar to the hepatocyte growth factor receptor. Fibrocystin is located in the primary cilium, basal body, and apical plasma membrane [6]. Recent studies have shown that fibrocystin undergoes proteolytic cleavage, releasing a C-terminal fragment that translocates to the nucleus [7, 8]. Fibrocystin also participates in a ciliary complex with polycystin-2, which is mutated in autosomal dominant polycystic kidney disease (ADPKD) and is involved in flow-stimulated intracellular calcium signaling [9].

Generation of a *Pkhd1* knockout mouse that mimics the human disease has been challenging. Deletion of exon 40 of *Pkhd1* produces biliary dysgenesis but does not cause kidney abnormalities [10]. Deletion of exon 2 results in proximal tubule dilatation in older females, but males are unaffected and no involvement of the collecting ducts is observed [11]. Deletion of exons 3–4 of *Pkhd1* produces cysts in the thick ascending limb and collecting duct cysts that usually appear after 3 months of age [12]. We targeted exons 1–3 of *Pkhd1*, which includes the site of the T36M mutation, to generate a model that may more closely replicate the human disease. Similar to humans with ARPKD, the mouse develops kidney cysts and ductal plate malformations and should be useful for our understanding of the pathogenesis of the disease. In addition, our model includes a *lacZ* reporter gene inserted at the *Pkhd1* locus, which will assist in the understanding of *Pkhd1* gene expression and promoter activity.

Materials and methods

Generation of $Pkhd1^{lacZ}$ mice

High-fidelity polymerase chain reaction (PCR) was used to amplify the proximal 2-kb *Pkhd1* promoter from a bacterial artificial chromosome (BAC) containing the *Pkhd1* gene (BAC354J18 from the Roswell Parker Cancer Institute (RPCI)-22 BAC genomic library). The PCR fragment was gel-purified and cloned into the *Kpn*I and *Xba*I sites upstream of the *lacZ* reporter gene in the plasmid pnLacF [13]. A targeting vector was created using the plasmid osdupdel, which contains a floxed neomycin resistance gene and thymidine kinase cassette [14]. The *Pkhd1/lacZ* cassette was released from pnLacF and cloned into the *Kpn*I and *Bam*HI sites of osdupdel, creating the short (5') arm of homology. Exons 4–5 of *Pkhd1* were amplified from the BAC and cloned into the *Spe*I and *Sfi*I sites of osdupdel, creating the long (3') arm of homology. The plasmid was linearized with *Spe*1 and purified. Embryonic stem (ES) cells (129Sv) were transfected with the *Pkhd1/lacZ* knock-in construct by the University of Texas (UT) Southwestern Transgenic Core Facility. ES cell clones were selected with G418/ganciclovir. Positive clones were identified by PCR and confirmed by Southern blot analysis. Successfully targeted cells were injected into C57BL/6J blastocysts and transferred into Institute Cancer Research (ICR) pseudo-pregnant foster mothers. The resulting chimeric animals were backcrossed with C57BL/6J for six generations. $Pkhd1^{lacZ/+}$ heterozygotes were intercrossed to generate homozygous $Pkhd1^{lacZ/lacZ}$ knockout mice. All experiments involving animals were conducted under the auspices of the UT Southwestern Institutional Animal Care and Use Committee.

Reverse transcriptase–polymerase chain reaction analysis

Total kidney RNA was extracted with Trizol reagent (Invitrogen). One microgram of RNA was treated with amp grade DNAaseI, and cDNA was synthesized with the use of Stratascript RT (Stratagene). PCR was performed with the following primers (conditions available on request):

Pkhd1 (exons 1–3): 5'-CATTTGAGGCACAAGGCT GACACA-3', 5'-TATGGCCCTGCATCTGCTTCTGAT-3'; *Pkhd1* (exons 10–11): 5'-GGGAGGTCGATGGTGCA TAAG-3', 5'-GATGTCCGTTCTTCCCCCAAG-3';

Pkhd1 (exons 34–36): 5'-GACAGAGTCAGTCTTTC CATCGTT-3', 5'-TTCGCATCAAGCAGTAGCAGG-3'; *Pkhd1* (exons 53–54): 5'-AAGTCAAGGGCCATCA CATC-3', 5'ATGTTTCTGGTCAACAGCCC-3'; *Pkd1*: 5'-GGTAGAGGCTGGCTCAGA-3', 5'-TGGGGTAGTG TAAATATGCG-3'; *Pkd2*: 5'-GTCGAAAACAGA GAAAACCAAC-3', 5'-ATGATCTCACAGGCTGC CAGG-3'

X-Gal and histological staining

We measured expression of β-galactosidase by staining with 5-bromo-4-chloro-3-indoyl β D-galactosidase (X-Gal, Stratagene), as described previously [15]. Briefly, adult tissues were perfused with ice-cold phosphate-buffered saline (PBS) followed by PBS containing 2% paraformaldehyde. The kidneys were bisected and immersed in 2% paraformaldehyde for 1 h. After fixation, tissue samples

were rinsed with PBS and incubated overnight at 4°C in PBS containing 30% sucrose. Cryoprotected samples were embedded in optimal cloning temperature (OCT) medium, frozen in liquid nitrogen, sectioned at 5–10 μm, and mounted on Vectabond-coated slides. The sections were incubated in staining solution [PBS containing 20 mM Tris-Cl (pH 7.4), 1.8 mM spermidine, 2 mM $MgCl_2$, 0.02% Nonidet P-40, 0.01% sodium deoxycholate, 5 mM potassium ferrocyanide, 5 mM potassium ferricyanide, and 1 mg/ml X-Gal]. Staining with X-Gal was performed at 37°C in the dark with continuous agitation. The sections were washed with PBS and counterstained with eosin (Sigma-Aldrich). The stained sections were rinsed with PBS and photographed under bright-field illumination using a Zeiss Axioplan 2 microscope. The paraffin-embedded sections were stained with hematoxylin and eosin according to standard protocols (UT Southwestern Molecular Pathology Core).

Antibody and lectin staining

Paraformaldehyde-fixed cryosections were stained with antibodies against aquaporin-3 (AQP3, Chemicon) and Na-K-Cl cotransporter 2 (NKCC2, Sigma) as described previously [16]. We conjugated the NKCC2 antibody, using a Zenon 488 labeling kit. Lectin staining was performed with fluorescein isothiocyanate-coupled *Lotus tetragonolo-*

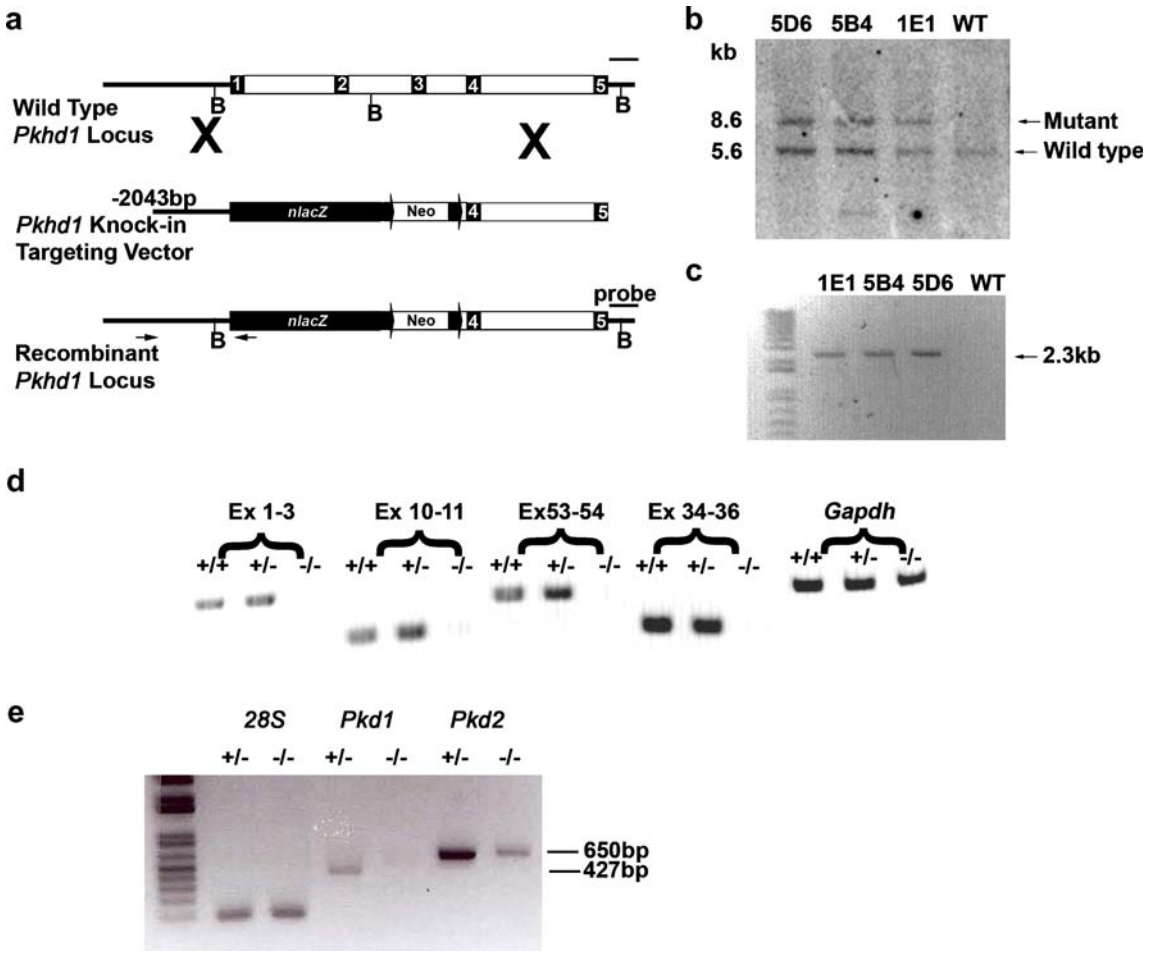

Fig. 1 *Pkhd1* knock-in strategy. **a** *Upper* Wild-type *Pkhd1* locus showing proximal promoter (*thick line*) and exons 1–5 (*boxes*). *Middle* *Pkhd1* targeting vector containing 2,043 bp of the proximal *Pkhd1* promoter, *lacZ* reporter gene with nuclear localization signal, inverted floxed neomycin resistance gene, and *Pkhd1* exons 4–5. *Lower* Recombinant locus showing replacement of *Pkhd1* exons 1–3 with the *lacZ* reporter gene. The *bar* indicates the probe for Southern blot analysis, and *arrows* indicate PCR primers used to confirm targeting. *B* *Bcl*I. **b** Southern blot analysis of ES cell clones 5D6, 5B4, and 1E1. The 5.5 kb band is present in the ES cells and wild-type DNA. The 8.6 kb band is seen only in the correctly targeted ES cells. **c** PCR confirming the targeting of *Pkhd1*. The 2.3 kb product was generated with an internal and external primer. **d** RT-PCR analysis of *Pkhd1* in the kidney. Primers were designed to amplify exons 1–3, 10–11, 53–54, and 34–36. *Pkhd1* transcripts were detected in wild-type (+/+) and heterozygous (+/−) mice but not in homozygous mice (−/−). *Gapdh* was used as a positive control. **e** RT-PCR analysis of *Pkd1* and *Pkd2* in the kidneys at P60. *Pkd1* and *Pkd2* transcript levels were diminished in homozygous mutant mice compared with heterozygous mice. 28S RNA was used as a positive control

bus agglutinin and *Dolichos biflorus* agglutinin (LTA and DBA, Vector Laboratories, Burlingame, CA, USA).

Biochemical studies

Whole blood was collected from anesthetized mice via retro-orbital venous puncture. The samples were incubated on ice then centrifuged at 4,000 r.p.m. for 10 min. The serum was aspirated and stored at 4°C. Serum alanine aminotransferase (ALT), aspartate aminotransferase (AST), gamma-glutamyltransferase (γGT) and blood urea nitrogen (BUN) were measured by the Mouse Metabolic Phenotyping Core at UT Southwestern Medical Center using a Vitros 250 chemical analyzer (Orthoclinical Diagnostics).

Results

Generation of *Pkhd1* knockout mice

A targeting vector was designed to replace exons 1–3 of *Pkhd1* with a *lacZ* reporter gene. The targeting vector contained 2,043 bp of the proximal *Pkhd1* promoter linked to a nuclear-localized *lacZ* reporter gene, followed by exons 4–5 of *Pkhd1* (Fig. 1a). The *lacZ* reporter gene contained a stop codon so that no fusion protein would be generated. ES cells were transfected with the plasmid and subjected to positive–negative selection with G418 and ganciclovir. Homologous recombination was confirmed by Southern blot analysis (Fig. 1b) and PCR using primers flanking the end of the targeting vector (Fig. 1c). Three successfully targeted ES cell clones were identified and injected into C57BL/6J blastocysts. Chimeric progeny were mated with C57BL/6J mice and backcrossed for six generations. Heterozygous $Pkhd1^{lacZ/+}$ mice and homozygous $Pkhd1^{lacZ/lacZ}$ mice were fertile and were used for breeding. Matings between $Pkhd1^{lacZ/+}$ heterozygotes produced the expected Mendelian ratios of homozygous mice. Figure 1d shows reverse transcriptase–polymerase chain reaction (RT-PCR) analysis of RNA extracted from the kidneys of wild-type, heterozygous, and homozygous mice. Primers from multiple regions of the gene were used to account for different *Pkhd1* transcripts generated by alternative splicing. The homozygous $Pkhd1^{lacZ/lacZ}$ mice did not express transcripts containing any of the amplified regions, whereas the heterozygous and wild-type mice expressed transcripts containing all the regions. These results indicated that $Pkhd1^{lacZ}$ was a null allele. Semi-quantitative RT-PCR analysis was performed to determine if the expression of other genes involved in polycystic kidney disease was altered in $Pkhd1^{lacZ/lacZ}$ mice. Figure 1e shows that the expression of *Pkd1* and *Pkd2* was diminished in homozygous mice compared with heterozygous mice.

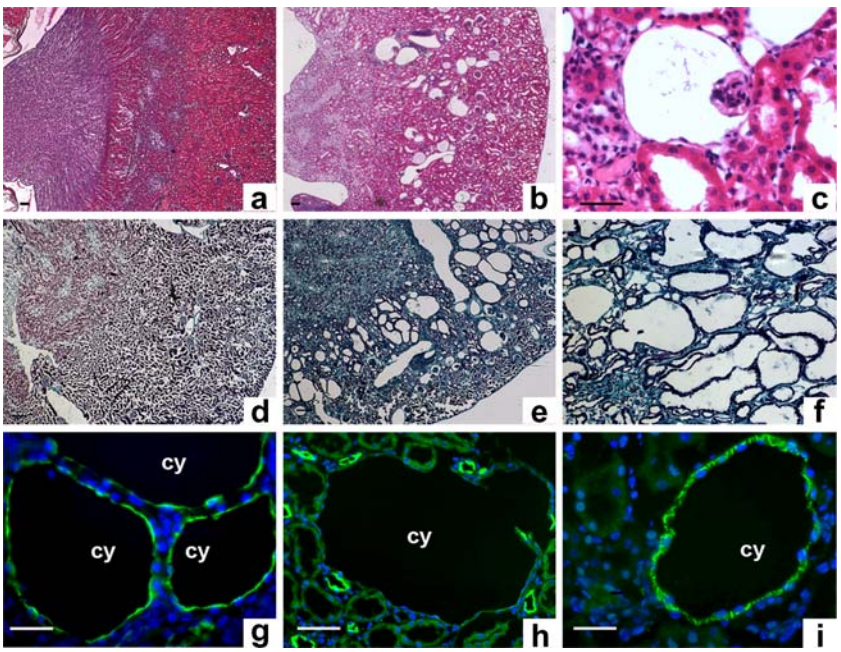

Fig. 2 Formation of kidney cysts in $Pkhd1^{lacZ/lacZ}$ mice. **a** Hematoxylin and eosin (H&E)-stained section of kidney from a 9-month-old wild-type mouse. **b** H&E-stained section of kidney from a 9-month-old $Pkhd1^{lacZ/lacZ}$ mouse. **c** Higher magnification image showing glomerular cysts and dilated tubules. **d** Trichrome-stained section of kidney from a 9-month-old $Pkhd1^{lacZ/+}$ mouse. **e** Trichrome-stained section of kidney from a 9-month-old $Pkhd1^{lacZ/lacZ}$ mouse. **f** Higher magnification image showing interstitial fibrosis and kidney cysts. **g–i** Kidney sections from a $Pkhd1^{lacZ/lacZ}$ mouse stained (*green*) with LTA (**g**) or antibodies to NKCC2 (**h**) and AQP3 (**i**). Nuclei were counterstained with 4′,6-diamidino-2-phenylindole (DAPI) (*blue*). *Bars* represent 50 μm. *cy* cyst

Pkhd1$^{lacZ/lacZ}$ mice develop cysts in proximal tubules, collecting ducts, and glomeruli

Heterozygous *Pkhd1*$^{lacZ/+}$ mice had normal-appearing kidneys (not shown). Homozygous *Pkhd1*$^{lacZ/lacZ}$ mice also had normal kidney morphology at birth but subsequently developed kidney cysts. Cyst formation was first observed when the mice were 45 days of age and progressed during adulthood. Both tubular and glomerular cysts were seen in adult homozygous mice (Fig. 2b,c) as opposed to the normal kidney histology seen in age-matched wild-type controls (Fig. 2a). Dilated tubules were found in both the renal cortex and medulla, but macrocysts were primarily located near the corticomedullary junction. Tubules were considered cystic if their diameters exceeded three-times that of the normal diameter [17]. A total of 69 *Pkhd1*$^{lacZ/lacZ}$ mice were analyzed. Severe cystic kidney disease was observed in 14/14 (100%) of homozygous *Pkhd1*$^{lacZ/lacZ}$ mice by the time they were 9 months of age. Trichrome staining showed that the kidney cysts in *Pkhd1*$^{lacZ/lacZ}$ mice were surrounded by areas of increased interstitial fibrosis when the mice were compared with age-matched *Pkhd1*$^{lacZ/+}$ mice (Fig. 2d–f). To identify the origins of the renal cysts, we stained the kidney sections with markers of specific nephron segments. The markers that were used were *Lotus tetragonolobus* agglutinin (LTA) for proximal tubules, Na-K-Cl cotransporter 2 (NKCC2) for thick ascending limbs, and aquaporin-3 (AQP3) for collecting ducts. Figure 2g shows multiple cortical cysts that were LTA-positive. Figure 2h shows that NKCC2 was absent in the cysts but was expressed in surrounding non-cystic tubules. Figure 2i shows a large cyst containing AQP3 in the basolateral membrane. These results indicated that the tubular cysts originated from proximal tubules and collecting ducts. Similar findings were observed in *Pkhd1*$^{lacZ/lacZ}$ mice after inbreeding on a 129SvEv background (data not shown). No sex differences were observed in the renal cystic phenotype of *Pkhd1*$^{lacZ/lacZ}$ mice.

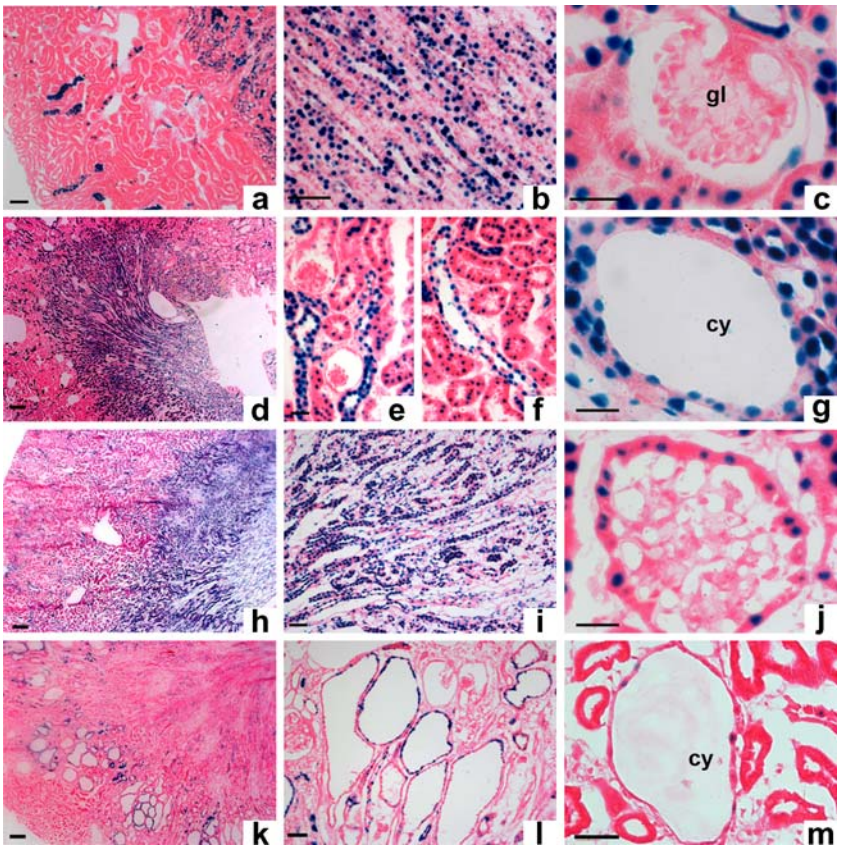

Fig. 3 *Pkhd1* promoter activity in kidney cysts. **a–c** X-Gal and eosin-stained kidney sections from *Pkhd1*$^{lacZ/+}$ mice showing β-galactosidase expression in medullary tubules (**b**) and Bowman's capsule (**c**). **d** X-Gal and eosin-stained sections from 45-day-old *Pkhd1*$^{lacZ/lacZ}$ mice, showing medullary and cortical cysts. **e** Higher magnification image of a glomerular cyst, showing absence of β-galactosidase expression. **f** Mildly dilated cortical collecting duct containing β-galactosidase-positive cells. **g** High-magnification image of a medullary cyst from a *Pkhd1*$^{lacZ/lacZ}$ mouse, showing β-galactosidase expression in cyst epithelial cells. **h–j** X-Gal and eosin-stained kidney sections from 9-month-old *Pkhd1*$^{lacZ/+}$ mice, showing β-galactosidase expression in medullary tubules (**l**) and Bowman's capsule (**j**). **k** X-Gal and eosin-stained section from a 9-month-old *Pkhd1*$^{lacZ/lacZ}$ mouse, showing cortical cysts and decreased expression of β-galactosidase in the medulla. **l–m** Higher magnification images of the cortex, showing decreased β-galactosidase expression in the tubular cysts and absence of expression in glomerular cysts. *Bars* represent 200 μm (**a, d, e, h, k**) and 50 μm (**b, c, f, g, i, j, l, m**). *gl* glomerulus, *cy* cyst

Decreased *Pkhd1* promoter activity in kidney cysts

We replaced exons 1–3 of *Pkhd1* with a *lacZ* reporter gene containing a nuclear localization signal. The resulting $Pkhd1^{lacZ}$ knock-in mice expressed β-galactosidase in the nuclei of cells under the control of the endogenous *Pkhd1* promoter and regulatory elements. Figure 3a shows the expression of β-galactosidase in the kidneys from an adult heterozygous $Pkhd1^{lacZ/+}$ mouse. β-Galactosidase was highly expressed in the nuclei of medullary collecting ducts (Fig. 3b). In the cortex, β-galactosidase was expressed in glomerular parietal epithelial cells and proximal tubules (Fig. 3c). No expression of β-galactosidase was observed in non-epithelial cells in the kidney.

Next, we examined β-galactosidase expression in cystic kidneys from homozygous $Pkhd1^{lacZ/lacZ}$ mice. When the mice were 45–60 days of age, large cortical and medullary macrocysts (Fig. 3d), glomerular cysts (Fig. 3e), and mildy dilated collecting ducts (Fig. 3f) were observed amongst numerous β-galactosidase-expressing proximal tubules and collecting ducts. The glomerular cysts did not express β-galactosidase (Fig. 3e), whereas β-galactosidase expression was detected in the cells lining the mildly dilated collecting ducts and cysts (Fig. 3f,g). When the mice were 9 months of age, the expression of β-galactosidase in the *Pkhd1* mutant mice had decreased in comparison with that of controls. Heterozygous $Pkhd1^{lacZ/+}$ mice continued to express β-galactosidase in collecting ducts, proximal tubules, and glomerular parietal epithelial cells (Fig. 3h,j). However, 9-month-old $Pkhd1^{lacZ/lacZ}$ mice showed dramatically lower β-galactosidase expression in the kidney (Fig. 3k). Many of the cyst epithelial cells did not express β-galactosidase, indicating loss of *Pkhd1* promoter activity at this stage (Fig. 3l,m). BUN levels were not significantly different in $Pkhd1^{lacZ/lacZ}$ knockout mice and wild-type mice at 3 months, 6 months, and 1 year of age (data not shown).

Ductal plate malformations and hepatic fibrosis in $Pkhd1^{lacZ/lacZ}$ mice

We performed histological analysis of the liver to determine the effect of loss of *Pkhd1* expression on biliary duct

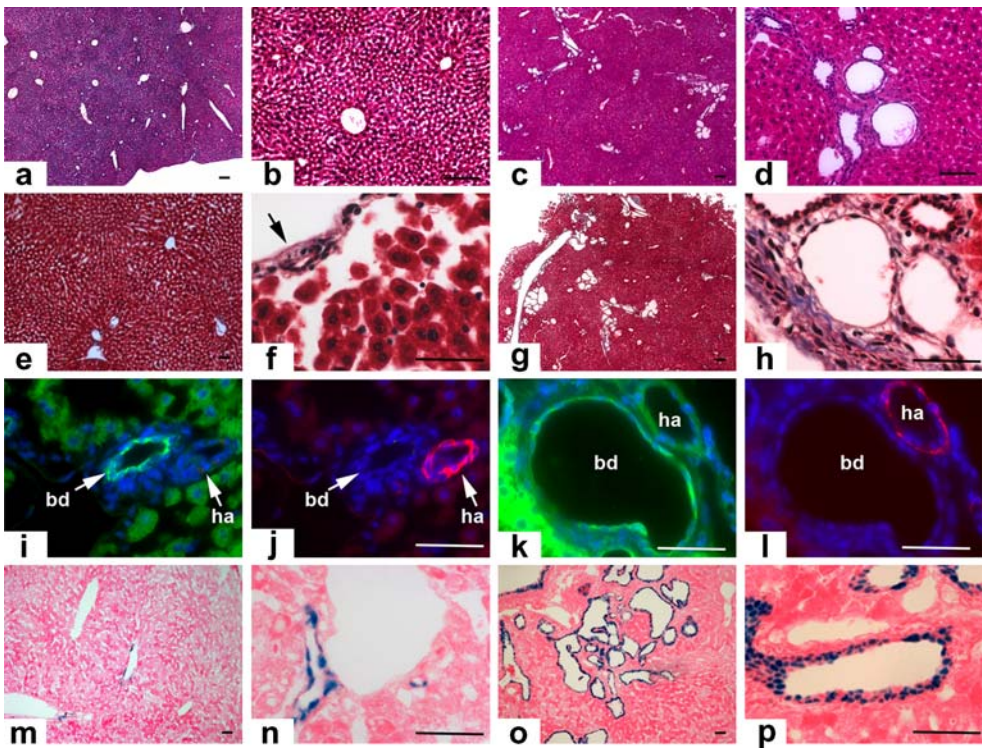

Fig. 4 Ductal plate malformations in $Pkhd1^{lacZ/lacZ}$ mice. **a** Hematoxylin and eosin (H&E)-stained section of the liver from a 2-month-old wild-type mouse. **b** High-magnification image of a central vein and portal tracts. **c** H&E-stained section of the liver from a 2-month-old $Pkhd1^{lacZ/lacZ}$ mouse, showing dilated irregular bile ducts. **d** Higher magnification image of a portal tract, showing multiple dilated bile ducts. **e, f** Trichrome-stained section of liver from an adult wild-type mouse. The *arrow* in **f** shows occasional blue staining, indicating fibrosis. **g, h** Trichrome-stained sections of livers from $Pkhd1^{lacZ/lacZ}$ mice, showing increased periportal fibrosis. **i–l** Sections of livers from wild-type mice (**i, j**) and $Pkhd1^{lacZ/lacZ}$ mice (**k, l**) stained for cytokeratin (*green*) and smooth muscle α-actin (*red*). **m, n** X-Gal and eosin-stained liver sections from $Pkhd1^{lacZ/+}$ mice, showing β-galactosidase expression in biliary epithelial cells. **o** X-Gal and eosin-stained liver section from a 60-day-old $Pkhd1^{lacZ/lacZ}$ mouse, showing β-galactosidase expression in dilated irregular bile ducts. **p** Dilated intra-hepatic bile ducts in $Pkhd1^{lacZ/lacZ}$ mice are lined by a multilayered epithelium. *Bars* represent 50 μm. *ha* hepatic artery, *bd* bile duct

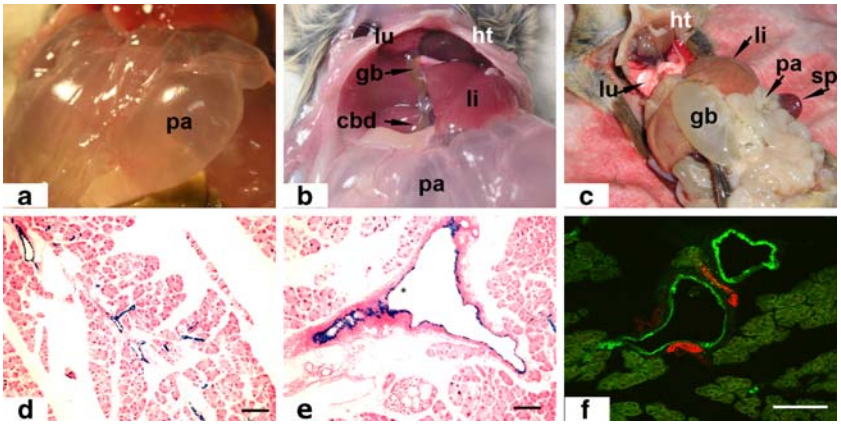

Fig. 5 Dilated pancreatic ducts and pancreatic and gall bladder cysts in *Pkhd1*$^{lacZ/lacZ}$ mice. **a** Gross pathology of the pancreas (*pa*) in a 2-month-old *Pkhd1*$^{lacZ/lacZ}$ mouse. **b** Massively cystic pancreas (*pa*) and normal-appearing common bile duct (*cbd*) and gall bladder (*gb*) in a 2-month-old *Pkhd1*$^{lacZ/lacZ}$ mouse. Lung (*lu*), liver (*li*), heart (*ht*). **c** Cystic gall bladder (*gb*) and splenomegaly (*sp*) in a *Pkhd1*$^{lacZ/lacZ}$ mouse. **d, e** X-Gal-stained sections of the pancreas from a *Pkhd1*$^{lacZ/+}$ mouse (**d**) and *Pkhd1*$^{lacZ/lacZ}$ mouse (**e**). **f** DBA staining (*green*) and anti-smooth muscle α-actin staining (*red*) show dilated pancreatic ducts in a *Pkhd1*$^{lacZ/lacZ}$ mouse. *Bars*, 100 μm

formation. The livers from *Pkhd1*$^{lacZ/lacZ}$ mice contained numerous dilated intrahepatic bile ducts (Fig. 4c) compared with those from wild-type, age-matched controls (Fig. 4a, b). The portal veins were surrounded by multiple dilated bile ducts that were lined by a multi-layered epithelium (Fig. 4d). The hepatocytes were morphologically normal. Periportal fibrosis, one of the hallmarks of liver involvement in ARPKD, was increased in *Pkhd1*$^{lacZ/lacZ}$ mice (Fig. 4e–h). Intrahepatic bile ducts were identified by expression of cytokeratin (Fig. 4i), and hepatic arteries were identified by smooth muscle actin expression (Fig. 4j). In *Pkhd1*$^{lacZ/lacZ}$ mice, the diameters of the intrahepatic bile ducts were much greater than those of the hepatic arteries (Fig. 4k,l), exceeding the 1:1.5 ratio seen in wild-type portal tracts [18]. β−Galactosidase expression was identified in intrahepatic bile ducts of heterozygous *Pkhd1*$^{lacZ/+}$ mice (Fig. 4m,n). In contrast to kidney cysts, *Pkhd1* promoter activity was unaffected in dilated intrahepatic bile ducts of homozygous mutant mice (Fig. 4o,p). No change in β-galactosidase expression was observed in the multi-layered biliary epithelial cells lining dilated, irregular, bile ducts in *Pkhd1*$^{lacZ/lacZ}$ mice. No significant differences in serum ALT, AST, and γGT levels were identified between homozygous *Pkhd1*$^{lacZ/lacZ}$ mice and wild-type controls (data not shown).

Pkhd1$^{lacZ/lacZ}$ mice develop pancreatic and gall bladder cysts

Gross and histological abnormalities were observed in the pancreases of *Pkhd1*$^{lacZ/lacZ}$ mice. Some mice developed large pancreatic cysts (Fig. 5a,b). In addition, dilatation of extrahepatic bile ducts and gall bladder cysts were observed in 2/12 (8%) of the *Pkhd1*$^{lacZ/lacZ}$ mice that were greater than 1 year old (Fig. 5c). Histologically, the pancreata in *Pkhd1*$^{lacZ/lacZ}$ mice showed dilated intra-acinar and inter-acinar exocrine ducts with diameters greater than three-times the normal diameter when compared with those of the *Pkhd1*$^{lacZ/+}$ heterozygotes (Fig. 5d,e). *Pkhd1* promoter activity was preserved in dilated ducts, as indicated by

Table 1 Abnormal phenotypes in *Pkhd1* knockout mouse (*tal* thick ascending limb)

Parameter	*Pkhd1*$^{lacZ/lacZ}$	*Pkhd1*$^{del2/del2}$ ref [11]	*Pkhd1*^{ex40} ref [10]	*Pkhd1*$^{del3\text{-}4/Del\ 3\text{-}4}$ ref [12]
Genetic background	C57BL/6J 129SvEv	C57BL/6J BALBc/J	C57BL/6J	C57BL/6J
Glomeruli	cysts	none	none	none
Proximal tubule	cysts	dilatation	none	none
tal	none	none	none	cysts
Collecting tubule	cysts	none	none	cysts
Portal tract	peri-portal fibrosis	peri-portal fibrosis	peri-portal fibrosis	peri-portal fibrosis
Intra-hepatic bile ducts	dilatation	dilatation	dilatation	dilatation
Pancreas	cysts	cysts	none	cysts
Gall bladder	cysts	none	none	cysts

the uniform β-galactosidase expression in the epithelial cells lining the dilated ducts. The dilated structures were identified as exocrine pancreatic ducts by immunohistochemical staining with DBA (Fig. 5f). Massive pancreatic cysts were identified in 7/69 (10%) of *Pkhd1*$^{lacZ/lacZ}$ mice.

Discussion

We deleted exons 1–3 of *Pkhd1* because this genomic region contains the transcription and translation start site. Deletion of exons 1–3 and replacement with a *lacZ* reporter gene resulted in the formation of kidney cysts originating from the glomerulus, proximal tubule, and collecting duct. The kidney phenotype of *Pkhd1*$^{lacZ/lacZ}$ mice is distinct from the phenotypes of the *Pkhd1* knockout mice that have been reported previously (Table 1). Female *Pkhd1*$^{del2/del2}$ mutant mice in which exon 2 has been deleted develop proximal tubular dilatation but no microcysts or macrocysts [11]. Male *Pkhd1*$^{del2/del2}$ mice have normal kidney histology. *Pkhd1*$^{del3–4/del3–4}$ mice that lack exons 3–4 develop cysts in the collecting ducts and thick ascending limb [12]. At 9 months of age, 50% of *Pkhd1*$^{del3–4/del3–4}$ mice had more than ten cysts per kidney, as opposed to 100% of *Pkhd1*$^{lacZ/lacZ}$ mice at the same age. No kidney cysts are seen in *Pkhd1*^{ex40} mice in which exon 40 has been deleted. The differences in the phenotypes are likely due to differences in the specific mutation of *Pkhd1* rather than differences in genetic background, since the mutant mice have been analyzed after inbreeding on a C57BL/6J background (Table 1).

Pkhd1$^{lacZ/lacZ}$ mice develop cysts in renal collecting ducts, similar to humans with ARPKD. Cysts are also found in proximal tubules, which are sites of transient cyst formation during fetal development in human ARPKD. However, in contrast to ARPKD, which frequently presents with severe neonatal disease, *Pkhd1*$^{lacZ/lacZ}$ mice are born with morphologically normal kidneys and do not develop cysts until adulthood. This phenotype more closely resembles that of humans with late-onset ARPKD. The severity of ARPKD can be highly variable, even between individuals with the same mutation, which may reflect influences of environmental factors or modifier genes. *Pkhd1*$^{lacZ/lacZ}$ mice develop glomerular cysts, a finding not previously reported in ARPKD and absent in the other *Pkhd1* knockout models. Studies using *Pkhd1*$^{lacZ/+}$ mice indicate that *Pkhd1* is expressed in Bowman's capsule. Hiesberger et al. recently showed that the expression of *Pkhd1* is regulated by the transcription factor hepatocyte nuclear factor (HNF)-1β [8]. Kidney-specific inactivation of HNF-1β in transgenic mice results in decreased expression of *Pkhd1* and formation of renal cysts [16]. Mutations of HNF-1β in humans are associated with glomerulocystic kidney disease. Taken together, these observations suggest that the formation of glomerular cysts in humans with HNF-1β mutations may be due to decreased expression of *Pkhd1*.

Since the *Pkhd1*$^{lacZ/lacZ}$ mice carry a *lacZ* reporter gene replacing exons 1–3, the expression of β-galactosidase reflects *Pkhd1* promoter activity. Heterozygous *Pkhd1*$^{lacZ/+}$ mice exhibit β-galactosidase expression in epithelial cells in the kidney, liver, and pancreas, consistent with the known pattern of expression of *Pkhd1*. *Pkhd1* promoter activity is preserved in cystic and non-cystic tubules in young homozygous *Pkhd1*$^{lacZ/lacZ}$ mice. In older mutant animals, *Pkhd1* promoter activity is diminished, and only a minority of cyst epithelial cells expresses β-galactosidase. Moreover, expression is also decreased in non-cystic tubules in the renal medulla. This observation suggests that the expression of *Pkhd1* is controlled by a transcriptional autoregulatory mechanism.

Pkhd1$^{lacZ/lacZ}$ mice exhibit progressive cyst formation that is manifested after the completion of postnatal nephrogenesis. This observation suggests that *Pkhd1* is not essential for tubulogenesis but is required for the maintenance of normal tubule architecture. Previous studies have shown that the *Pkhd1* gene product, fibrocystin, interacts in a complex with polycystin-2, and the two proteins together regulate flow-induced intracellular calcium release [9, 19]. Fibrocystin, in turn, undergoes calcium-dependent proteolytic cleavage and translocates to the nucleus, where it may participate in gene transcription [20]. Kidneys from homozygous *Pkhd1*$^{lacZ/lacZ}$ mice have diminished expression of *Pkd1* and *Pkd2*. This alteration in gene expression is not seen in kidneys from *Pkhd1*$^{del3–4/del3–4}$ mice; however, mice carrying mutations of both *Pkhd1* and *Pkd1* exhibit more severe cystic kidney disease than mice with mutations of *Pkhd1* by itself [12]. Taken together, these findings suggest the existence of a transcriptional relationship between *Pkhd1*, *Pkd1*, and *Pkd2*.

Dilated, irregular, intrahepatic bile ducts are consistently seen in homozygous mutant *Pkhd1*$^{lacZ/lacZ}$ mice. This lesion resembles the classical ductal plate malformation seen in humans with ARPKD. A similar hepatic phenotype has been observed in *Pkhd1*$^{del3–4/del3–4}$, *Pkhd1*^{ex40} *and* *Pkhd1*$^{del2/del2}$ mice. *Pkhd1*$^{lacZ/lacZ}$ mice, *Pkhd1*$^{del2/del2}$ mice, and *Pkhd1*$^{del3–4/del3–4}$ mice also develop cysts in the exocrine ducts of the pancreas. Pancreatic duct dilatation and cysts have not been reported in ARPKD, although fibrosis of the pancreas has been described. Pancreatic disease was not observed in the *Pkhd1*^{ex40} mouse, which may reflect the persistent expression of a fibrocystin mutant lacking 63 amino acids, whereas *Pkhd1*^{lacZ} is a null allele.

Acknowledgments This work was supported by National Institutes of Health (NIH) grants R01DK42921 and R01DK67565 and the UT

Southwestern O'Brien Kidney Research Core Center (NIH P30DK079328).

References

1. Igarashi P, Somlo S (2002) Genetics and pathogenesis of polycystic kidney disease. J Am Soc Nephrol 13:2384–2398
2. Adeva M, El-Youssef M, Rossetti S, Kamath PS, Kubly V, Consugar MB, Milliner DM, King BF, Torres VE, Harris PC (2006) Clinical and molecular characterization defines a broadened spectrum of autosomal recessive polycystic kidney disease (ARPKD). Medicine (Baltimore) 85:1–21
3. Ward CJ, Hogan MC, Rossetti S, Walker D, Sneddon T, Wang X, Kubly V, Cunningham JM, Bacallao R, Ishibashi M, Milliner DS, Torres VE, Harris PC (2002) The gene mutated in autosomal recessive polycystic kidney disease encodes a large, receptor-like protein. Nat Genet 30:259–269
4. Nagasawa Y, Matthiesen S, Onuchic LF, Hou X, Bergmann C, Esquivel E, Senderek J, Ren Z, Zeltner R, Furu L, Avner E, Moser M, Somlo S, Guay-Woodford L, Buttner R, Zerres K, Germino GG (2002) Identification and characterization of Pkhd1, the mouse orthologue of the human ARPKD gene. J Am Soc Nephrol 13:2246–2258
5. Bergmann C, Senderek J, Sedlacek B, Pegiazoglou I, Puglia P, Eggermann T, Rudnik-Schoneborn S, Furu L, Onuchic LF, De Baca M, Germino GG, Guay-Woodford L, Somlo S, Moser M, Buttner R, Zerres K (2003) Spectrum of mutations in the gene for autosomal recessive polycystic kidney disease (ARPKD/PKHD1). J Am Soc Nephrol 14:76–89
6. Ward CJ, Yuan D, Masyuk TV, Wang X, Punyashthiti R, Whelan S, Bacallao R, Torra R, LaRusso NF, Torres VE, Harris PC (2003) Cellular and subcellular localization of the ARPKD protein; fibrocystin is expressed on primary cilia. Hum Mol Genet 12:2703–2710
7. Kaimori JY, Nagasawa Y, Menezes LF, Garcia-Gonzalez MA, Deng J, Imai E, Onuchic LF, Guay-Woodford LM, Germino GG (2007) Polyductin undergoes notch-like processing and regulated release from primary cilia. Hum Mol Genet 16:942–956
8. Hiesberger T, Shao X, Gourley E, Reimann A, Pontoglio M, Igarashi P (2005) Role of the hepatocyte nuclear factor-1beta (HNF-1beta) C-terminal domain in Pkhd1 (ARPKD) gene transcription and renal cystogenesis. J Biol Chem 280:10578–10586
9. Wang S, Zhang J, Nauli SM, Li X, Starremans PG, Luo Y, Roberts KA, Zhou J (2007) Fibrocystin/polyductin, found in the same protein complex with polycystin-2, regulates calcium responses in kidney epithelia. Mol Cell Biol 27:3241–3252
10. Moser M, Matthiesen S, Kirfel J, Schorle H, Bergmann C, Senderek J, Rudnik-Schoneborn S, Zerres K, Buettner R (2005) A mouse model for cystic biliary dysgenesis in autosomal recessive polycystic kidney disease (ARPKD). Hepatology 41:1113–1121
11. Woollard JR, Punyashtiti R, Richardson S, Masyuk TV, Whelan S, Huang BQ, Lager DJ, vanDeursen J, Torres VE, Gattone VH, LaRusso NF, Harris PC, Ward CJ (2007) A mouse model of autosomal recessive polycystic kidney disease with biliary duct and proximal tubule dilatation. Kidney Int 72:328–336
12. Garcia-Gonzalez MA, Menezes LF, Piontek KB, Kaimori J, Huso DL, Watnick T, Onuchic LF, Guay-Woodford LM, Germino GG (2007) Genetic interaction studies link autosomal dominant and recessive polycystic kidney disease in a common pathway. Hum Mol Genet:16:1940–1950
13. Kapur RP, Hoyle GW, Mercer EH, Brinster RL, Palmiter RD (1991) Some neuronal cell populations express human dopamine [beta]-hydroxylase-lacZ transgenes transiently during embryonic development. Neuron 7:717–727
14. Wang Y, Spatz MK, Kannan K, Hayk H, Avivi A, Gorivodsky M, Pines M, Yayon A, Lonai P, Givol D (1999) A mouse model for achondroplasia produced by targeting fibroblast growth factor receptor 3. Proc Natl Acad Sci U S A 96:4455–4460
15. Igarashi P, Shashikant CS, Thomson RB, Whyte DA, Liu-Chen S, Ruddle FH, Aronson PS (1999) Ksp-cadherin gene promoter. II. Kidney-specific activity in transgenic mice. Am J Physiol Renal Physiol 277:F599–F610
16. Hiesberger T, Bai Y, Shao X, McNally BT, Sinclair AM, Tian X, Somlo S, Igarashi P (2004) Mutation of hepatocyte nuclear factor-1beta inhibits Pkhd1 gene expression and produces renal cysts in mice. J Clin Invest 113:814–825
17. Wu G, Tian X, Nishimura S, Markowitz GS, D'Agati V, Hoon Park J, Yao L, Li L, Geng L, Zhao H, Edelmann W, Somlo S (2002) Trans-heterozygous Pkd1 and Pkd2 mutations modify expression of polycystic kidney disease. Hum Mol Genet 11:1845–1854
18. Crawford AR, Lin XZ, Crawford JM (1998) The normal adult human liver biopsy: a quantitative reference standard. Hepatology 28:323–331
19. Wu Y, Dai X-Q, Li Q, Chen CX, Mai W, Hussain Z, Long W, Montalbetti N, Li G, Glynne R, Wang S, Cantiello HF, Wu G, Chen X-Z (2006) Kinesin-2 mediates physical and functional interactions between polycystin-2 and fibrocystin. Hum Mol Genet 15:3280–3292
20. Hiesberger T, Gourley E, Erickson A, Koulen P, Ward CJ, Masyuk TV, Larusso NF, Harris PC, Igarashi P (2006) Proteolytic cleavage and nuclear translocation of fibrocystin is regulated by intracellular Ca2+ and activation of protein kinase C. J Biol Chem 281:34357–34364